Acta Crystallographica Section D
Biological Crystallography
ISSN 0907-4449

Nonstoichiometric complex of gramicidin D with KI at 0.80 Å resolution

A. Olczak,[a] M. L. Główka,[a]* M. Szczesio,[a] J. Bojarska,[a] W. L. Duax,[b,c] B. M. Burkhart[b] and Z. Wawrzak[d]

[a]Institute of General and Ecological Chemistry, University of Technology, Łódź, Poland, [b]Hauptman–Woodward Medical Research Institute, Buffalo, NY, USA, [c]State University of New York at Buffalo, Buffalo, NY, USA, and [d]Department of Biochemistry, Molecular Biology and Cell Biology, Northwestern University, 2205 Tech Drive, Evanston, Illinois 60208-3500, USA

Correspondence e-mail: marekglo@p.lodz.pl

Received 1 August 2006
Accepted 11 December 2006

PDB Reference: gramicidin D with KI, 2izq, r2izqsf.

The crystal structure of a nonstoichiometric complex of gramicidin D (gD) with KI has been determined at 100 K using synchrotron radiation. The final *R* factor was 0.106 for 83 988 observed reflections (Friedel pairs were not merged) collected to 0.80 Å. The structure consists of four independent pentadecapeptides and numerous solvent molecules and salt ions. The general architecture of the antiparallel double-stranded gramicidin dimers in the crystal (a right-handed antiparallel $DS\beta H_R$ form) closely resembles that of previously published cation complexes of gD. However, a significantly different mixture of gramicidin isomers is found in the crystal of the KI complex, including partial occupancy of phenylalanine at position 11. Only three sites in each of the two crystallographically independent channels are partially occupied by potassium cations instead of the commonly observed seven sites. The sum of the partial occupancies of K^+ (1.10 per two dimers) is consistent with the sum of the iodide occupancies (1.095 over eight sites), which is also confirmed by the anomalous signal of the iodide. There was a significant asymmetry of the distribution and occupancies of cations in the crystallographically independent gramicidin channels, in contrast to the distribution found in the rubidium chloride complex with gD.

1. Introduction

Gramicidin, being a relatively simple and easily accessible ionophoric compound, is a convenient model for studying the structure and function of ionic channels. As the antibacterial activity of gramicidin against Gram-positive species results from its ability to transport monovalent cations (especially sodium and potassium) across the cell membrane, knowledge of the crystal structures of gramicidin complexes containing cations is of great importance. Gramicidin has been reported to have several forms in solution, depending on the solvent conditions (Burkhart, Gassmann *et al.*, 1998). In the crystal state at least five distinct forms have been reported, including three cation-free forms: (i) a left-handed antiparallel double-stranded dimer studied by Langs (1988) (in orthorhombic crystals from ethanol), (ii) its monoclinic modification crystallized from methanol (Langs *et al.*, 1991) and (iii) an antiparallel double-stranded right-handed dimer from acetic acid (Burkhart, Li *et al.*, 1998).

The two other forms comprise the complexed gramicidin reported in a number of crystal structures published to date, *i.e.* left-handed structures with CsCl (Wallace & Ravikumar, 1988) and KSCN (Wallace *et al.*, 1990; Doyle & Wallace, 1997) and several right-handed structures with CsCl (Burkhart, Li *et al.*, 1998), with RbCl (Główka *et al.*, 2005) and with CsCl,

$TlNO_3$, RbCl, KCl, KI and KSCN (Duax *et al.*, 2003). All of them, both left-handed and right-handed, belong to the same space group $P2_12_12_1$, with almost identical unit-cell parameters, and consist of antiparallel double-stranded dimers containing monovalent cations. Helical gramicidin dimers are stacked along the [001] direction and are linked by intermolecular hydrogen bonds, thus forming two crystallographically independent infinite channels, the axes of which overlap with a 2_1 screw axis. To date, the atomic coordinates for three cation-free forms, two left-handed forms (1c4d and 1gmk) and two right-handed complexed forms (1av2 and 1w5u), have been deposited in the PDB (Berman *et al.*, 2000).

The left-handed structures of complexed gramicidin (Wallace & Ravikumar, 1988; Wallace *et al.*, 1990; Doyle & Wallace, 1997) have many characteristics that are typical of an incorrect structure determination, including the exclusion of diffraction data recorded in the range 2.5–2.0 Å from the refinement, the overlap of some Trp side chains, the unfavourable positions of side chains on the Ramachandran plot in the KSCN complex and the placement of Cs^+ outside and Cl^- inside the channel in the case of the CsCl complex. For a more detailed discussion, see Burkhart, Li *et al.* (1998).

The importance of potassium cations in cell function and disagreement over the handedness of the helices in known gramicidin complexes led us to study the potassium iodide complex at higher resolution using synchrotron-radiation data. The presence of iodide in the crystals allowed us to use its anomalous diffraction signal to reliably locate anion positions and to determine the nature of their interaction with gramicidin side chains.

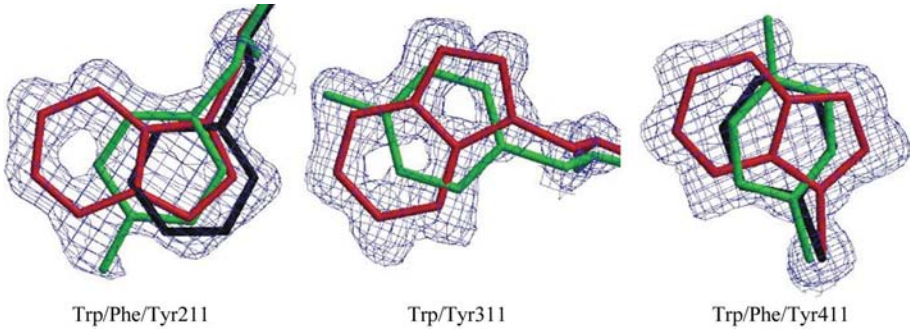

Figure 1
Trp/Phe/Tyr residues at positions 211 and 411 and Trp/Tyr at 311 with superimposed $2F_o - F_c$ (blue) maps at the 1σ level. The populations of Trp, Phe and Tyr residues in all positions 11 are shown in Table 3.

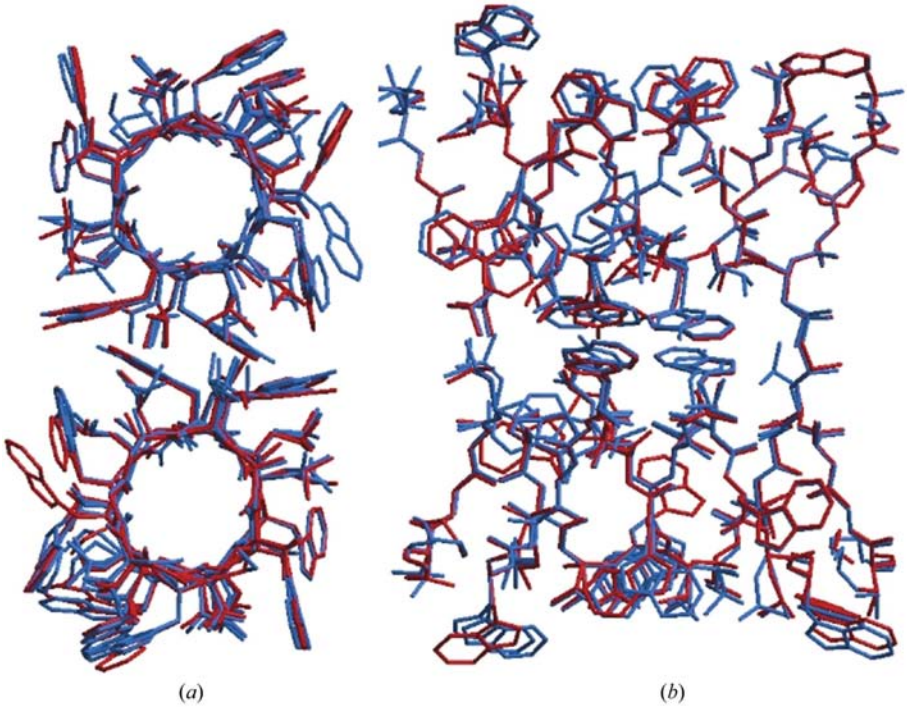

Figure 2
Conformations of side chains in the crystal structures of the RbCl complex (red) and KI complex (blue) shown down the [001] direction (*a*) and along the [001] direction (*b*). This figure was prepared with *RASTER3D* (Merritt & Murphy, 1994).

We have used wild-type gramicidin D for crystallization in order to acquire additional data (Burkhart, Gassmann *et al.*, 1998) on the possible role of heterodimers in the nucleation of gramicidin crystals and the effect of solvent on crystal composition. Wild-type gramicidin D is a mixture of gramicidin A, B and C in approximate proportions of 80:5:15 (Sarges & Witkop, 1965; Hladky & Haydon, 1970; Weinstein *et al.*, 1980). The three isomers differ in the aromatic substitution at position 11, which is tryptophan, phenylalanine and tyrosine in gramicidin A, B and C, respectively. Position 1 is occupied by two possible residues, Val or Ile, in a ratio of about 85:15 (Hotchkiss, 1944).

The isotropic organic solvents used for the crystallization of gramicidin and its complexes do not resemble the heterogeneous nature of the membrane environment. Other modifications of a gramicidin dimer have been proposed on the basis of biochemical data. The conformation most often postulated to be responsible for biological activity is a single-stranded head-to-head dimer first proposed by Urry (1971), with its tryptophans gathered on both ends of the gramicidin channel buried in the lipophilic cell membrane. Such an arrangement enables these more hydrophilic residues (capable of hydrogen-bond formation) to approach the water phases on both sides of the membrane. All attempts to crystallize an antiparallel single-stranded gramicidin dimer have failed.

2. Materials and methods

2.1. Crystallization and data collection

Commercially available gramicidin D (Sigma) and analytical grade KI and methanol were used in simple batch crystallization. For cryotemperature (100 K) data collection, a single crystal of the gD–KI complex was picked up in a fiber loop, immersed in a glycerol/water (3:1) solution for a few seconds, scooped out in another loop mounted on a diffractometer pin and placed in a transportation tank under liquid nitrogen. The diffraction data were collected on the 5-ID beamline of DND-CAT at the Advanced Photon Source, Argonne, IL, USA using a 165 mm MAR CCD detector and were processed with the *HKL* software package (Otwinowski & Minor, 1997). Diffraction data were recorded to 0.80 Å resolution using a wavelength of 0.67 Å. Table 1 shows details of the experiment.

2.2. Structure refinement

The method of determination of the gD–CsCl complex structure has been described in detail in Burkhart, Li *et al.* (1998). The right-handed Burkhart model has none of the anomalies present in the Wallace model and was taken as the starting model in this study. The model was refined using the *SHELX*97 package (Sheldrick & Schneider, 1997) with conjugate-gradient least squares (CGLS). Anisotropic refinement with manual adjustment enabled the detection of gC and gB components (Fig. 1) and disorder in many side chains, the identification of additional solvent molecules and ions and the refinement of their occupancy factors. The multiple-conformation site-occupancy factors for side chains were refined constraining their sum to be unity. The occupancy factors of K^+ and water molecules in the channels and some I^- ions were unrestrained during refinement. H-atom positions were refined in riding positions on their parent atoms. Engh & Huber (1991) restraints on bond distances and angles were used in refinements. The weighting scheme used was $w^{-1} = \sigma^2(F_o^2) + (aP)^2$, where $a = 0.29$ and $P = 1/3[2F_c^2 + \max(F_o^2, 0)]$.

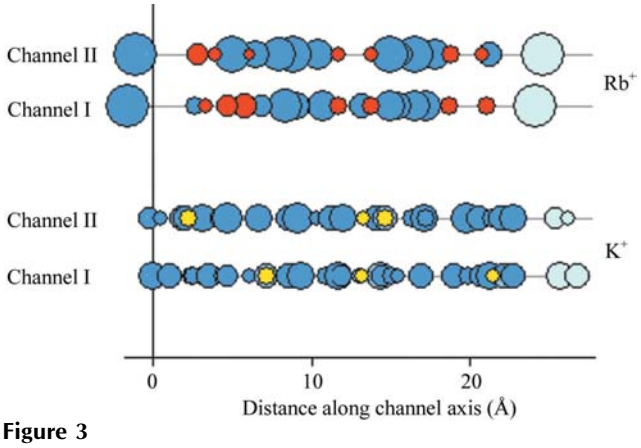

Figure 3
Distribution of K^+ ions (yellow circles), Rb^+ ions (red circles) and waters (blue circles) in gramicidin channels I and II in the crystal structures of the gD–KI and gD–RbCl complexes, shown along the channel axis. The circle area size is proportional to the occupancy factor. Light blue circles represent water molecules in the neighboring dimers. The origin is at the C^α1 atom of strands 100 and 300.

Table 1
Crystal data, solution and refinement statistics.

Values in parentheses are for the highest resolution shell (0.83–0.80 Å).

Crystal data	
Formula of main component (gA)	$C_{99}H_{140}N_{20}O_{17}$
Molecular weight of gA (Da)	1882.3
Crystal system	Orthorhombic
Formula units Z	16 [$Z' = 4$]
Crystal dimensions (mm)	0.40 × 0.35 × 0.20
Linear absorption coefficient (mm^{-1})	0.22
Radiation source	Synchrotron
Wavelength (Å)	0.67
Crystallographic data-collection details	
Space group	$P2_12_12_1$
Unit-cell parameters (Å)	a = 30.144, b = 31.319, c = 51.550
Unit-cell volume ($Å^3$)	48667.3
No. of unique reflections measured	51435
R_{merge} (%)	8.1 (28.5)
No. of observed reflections [$>2\sigma(I)$]	47081
$I/\sigma(I)$	16.7 (6.2)
Resolution range (Å)	26.5–0.80
Completeness (%)	98.17 (99.55)
Refinement statistics and other details	
No. of restraints	15555
No. of parameters	8994
Final R_{free}(%)	0.116
Final R_1 (%)	0.106
Final R_1, all data (%)	0.110 [51435 reflections]
wR^2	0.3071
Goodness of fit (GooF)	1.028
$\Delta\rho$ (max, min) (e $Å^{-3}$)	0.97, −0.34

2.3. Potassium positions

In contrast to the rubidium complex (Główka *et al.*, 2005), the potassium positions in this structure could not be identified on the basis of anomalous scattering signal alone. Only the two with the highest occupancies appeared in the anomalous difference map. Distinguishing potassium ions with lower occupancies (atomic No. 19) from the water (ten electrons) present in the crystal was not easy owing to the partial occupancies of both species. To distinguish between the two species, we have refined the structure with many possible compositions and compared the results, including the atomic displacement parameters (isotropic after refinement with free occupancy), the anisotropy of B and careful analysis of the coordination sphere.

3. Results and discussion

The final refined model of the structure consists of over 540 non-H atoms present in gA, 27 water sites, 14 KI ion sites and five methanol molecules. In addition, a significant amount of gC (26%) and a detectable content of gB (about 6.75%) were found, increasing the number of sites being refined to 978, excluding H atoms. 1.10 (1) K^+ and 1.095 (7) I^- ions were also identified distributed over six (K^+) and eight (I^-) sites (Table 2).

There are four crystallographically independent molecules of gramicidin in the studied crystal, forming two pairs of

Table 2
Occupancies and atomic displacement parameters of ions as found in this study.

Ion	Occupancy	B (Å^2)
K1	0.190 (5)	5.19 (11)
K2	0.166 (5)	6.27 (15)
K3	0.143 (5)	6.33 (15)
K11	0.207 (6)	8.26 (16)
K12	0.157 (4)	5.72 (12)
K13	0.238 (7)	6.17 (12)
I21	0.231 (1)	4.68 (2)
I22	0.203 (1)	5.53 (4)
I23	0.119 (2)	6.94 (7)
I24	0.181 (2)	8.01 (8)
I25	0.087 (2)	11.34 (20)
I26	0.102 (2)	11.46 (18)
I27	0.116 (2)	10.78 (15)
I28	0.056 (2)	9.62 (23)

helical right-handed strands intertwined in an antiparallel fashion. The dimers are stacked along the [001] direction and are linked by two intermolecular hydrogen bonds, thus forming two crystallographically independent infinite channels, the axes of which overlap with the 2_1 screw axis. The numbering system for amino acids, polypeptide strands, gramicidin dimers (channels) and other residues followed that used in the description of the gD–RbCl complex. Geometrical analysis was carried out with the *CCP*4 suite (Collaborative Computational Project, Number 4, 1994), *PROCHECK* (Laskowski *et al.*, 1993) and *XFIT* (McRee, 1999).

3.1. Gramicidin double-stranded dimers

Although the gramicidin D used in this study came from the same source as that used in the crystallization of the RbCl complex and the crystallization conditions were the same except for the solvent used (ethanol instead of methanol), the composition of the gramicidin in the crystal studied differs significantly (Table 3) from that found in the RbCl complex. In the RbCl complex the gramicidin composition was 89.5% gA and 10.5% gC, while in the KI complex the values are 67.25% and 26.0%, respectively, very different from those in the gramicidin D used for crystallization (80% and 15%, respectively; Sarges & Witkop, 1965; Hladky & Haydon, 1970; Weinstein *et al.*, 1980). Although 6.75% of the gB component has been detected in the KI complex, it is only present in two of the four strands (200 and 400; Table 3). No gB component was detected in the RbCl complex and gramicidin C was also only observed in strands 200 and 400. A similar observation of increased gC content in crystals of gramicidin complexes was reported by Burkhart, Gassman *et al.* (1998), who made a more detailed analysis of the phenomenon and suggested that the heterogenity of the gramicidin channels plays an important role in nucleation and crystal packing.

The conformations of the main chains, as defined by the ψ and φ angles, do not show any unusual features. On the other hand, the side chains in this study show a higher heterogeneity of their conformations (Table 4) compared with those found in the rubidium complex. This may result from the higher resolution of the KI structure, which enables the identification of conformers with lower occupancies. The conformations of the side chains in the two crystallographically independent dimers are generally similar (Fig. 2).

Table 3
Heterogeneity (%) of gramicidin D complexes resulting from different residues present at position 11: Trp in gA, Phe in gB and Tyr in gC.

The composition of the gD used in the crystallization was ~80% gA, ~5% gB, ~15% gC (Sarges & Witkop, 1965; Hladky & Haydon, 1970; Weinstein *et al.*, 1980).

	gD–RbCl†			gD–KI‡		
Residue	gA	gB	gC	gA	gB	gC
111	100	—	—	75	—	25
211	77	—	23	50	15	35
311	100	—	—	74	—	26
411	81	—	19	70	12	18

† As determined from the X-ray structure at 1.14 Å resolution (Główka *et al.*, 2005), in which neither gB nor Ig (Ile1 gramicidin) was detected. ‡ This study.

3.2. Gramicidin-channel contents

The most surprising features of the inside of the gramicidin channel were the small number of K^+-binding sites detected, the low potassium-ion content and an almost continuous stream of water observed in the crystal (Fig. 3, Table 5). Only three K^+ sites in each crystallographically independent channel have been unequivocally identified, which is quite different from the number of cationic sites (seven) found in the rubidium chloride complex and other crystal structures of right-handed gramicidin D complexes (Burkhart *et al.*, 1999). The smaller number of potassium sites in the channel compared with heavier cations (Burkhart, Li *et al.*, 1998) correlates with the lower affinity of the potassium cation for the gramicidin channel as evidenced by the higher conductance of this cation (Roux & Karplus, 1994). Another explanation would be the uncertainty of K^+ identification, since all sites were occupied only partially (statistically). However, the content of potassium after refinement with unrestrained occupation factors (1.10) matches the value of 1.095 found for the sum of the population of iodide ions (Table 2), which were easily identified owing to their higher atomic number and anomalous signal (§4).

Another difference in binding between the Rb and K complexes of gramicidin is the large deviation of K^+ positions from the channel axis. The average deviation is 0.74 and 0.72 Å for channels I and II, respectively. The potassium cations are closer to the channel wall (Table 6 and Fig. 4). There are usually two shorter contacts with two amino-acid carbonyl groups with K$\cdots$O distances below 3 Å and K$\cdots$O=C angles larger than 120° and two (more distant) K$\cdots\pi$(C=O) contacts with K$\cdots$O=C angles smaller than 120°, usually in the range 100–110° (Table 6). A similar regularity was observed for some cationic sites in the RbCl complex, but was less pronounced as a consequence of the larger Rb^+ diameter.

Table 4
Side-chain conformations (χ_1) in the crystal structures of right-handed double-stranded gramicidin complexes.

The older *gauche*/*trans* (g^+ or g^- and *t*; ac means anticlinal) notation has been used for simplicity. The population (%) of a conformer along the $C^\alpha-C^\beta$ bond with the higher value is shown. In the case of three orientations, the two higher values are shown. An asterisk (*) indicates positional disorder for strand 2.

Residue	Strand 1	Strand 2	Strand 3	Strand 4
gD–KI (this work)				
Val1	g^- (35), g^+ (35), g^-	g^+ (77), *t*	ac (51), g^+	*t*
D-Val6	*t* (50), g^+	*t* (50), g^+	g^- (68), g^+	g^- (55), *t*
Val7	g^-	g^+ (50), g^-	g^+ (53), g^-	g^- (52), *t*
D-Val8	ac$^-$ (50), *t* (25), g^+	*t*	g^+ (50), *t* (40), g^+	g^+ (66), *t*
D-Leu4	g^+ (65), *t*	g^+ (41), g^+	g^+ (39), *t* (31), g^+	g^- (87), g^+
D-Leu10	*t* (41), g^-	g^+ (40), g^- (30), g^+	g^+ (59), g^+	g^- (40), g^- (30), ac$^+$
D-Leu12	g^- (74), *t*	ac (65), g^+	*t* (55), *t*	g^- (75), g^-
D-Leu14	*t* (73), *t*	*t* (70), g^-	*t* (59), *t*	g^- (75), g^-
Trp9	g^- (37), *t*	g^- (74), g^-	g^- (65), g^-	g^- (52), g^-
Trp11/(Tyr)	g^- (75), (Tyr g^-)	g^- (50), (Tyr g^- 35)	g^- (74), (Tyr g^-)	g^- (70), (Tyr g^- 18)
Trp13	*t*	g^- (66), g^-	*t*	g^-(66), g^-
Trp15	*t*	g^- (56), g^-	*t* (58), *t*	g^- (83), g^-
gD–RbCl (Główka *et al.*, 2005)				
Val1	g^+	*t*	g^+	*t*
D-Val6	g^+ (77), *t*	*t*	g^+ (58), *t*	*t* (54), g^+
Val7	g^-	g^+ (57), g^-	g^- (55), g^+	g^+
D-Val8	g^+	*t*	g^- (61), g^+	g^- (68), *t*
D-Leu4	g^+ (58), *t*	g^+	*t*	g^+
D-Leu10	g^- (54), g^+	g^- (78), *t*	g^+	g^- (66), g^+
D-Leu12	*t*	g^- (66), g^+	**t* (55)	g^-
D-Leu14	*t*	*t* (78), g^+	*t*	g^-
Trp9	g^-	g^-	g^- (61), *t*	g^-
Trp11/(Tyr)	g^-	**g*− (24)	g^-	**g*$^-$ (19)
Trp13	*t*	**g*$^-$ (52)	*t*	**g*$^-$ (52)
Trp15	*t*	g^-	**t* (65)	g^-

The significantly smaller number of binding sites identified in this study compared with the RbCl complex correlates with the lower average cation content (0.50 and 0.60 in channels I and II, respectively) and the larger number of water sites and greater water content in the channels (Table 5). The resulting water-to-cation ratios for the two channels are 16.8 and 14.0, respectively, which are significantly higher than those in the RbCl complex (3.5 and 5.8, respectively; Główka *et al.*, 2005).

3.3. Interchannel space contents

Owing to the anomalous scattering of iodine, eight sites occupied by anions were easily identified in the anomalous difference Fourier map. The locations are roughly evenly distributed in the interchannel space, with occupancies ranging from 0.06 to 0.23 and B_{eq} values ranging from 4.7 to 11.5 Å^2. The total I^- occupancy in the asymmetric unit is 1.095, *i.e.* the same as the total K^+ occupancy of 1.10 (Table 2). In addition to the eight anionic sites, 32 water sites occupied by a total of 10.3 molecules and nine methanol sites (about five molecules) have been found in the interchannel space.

As expected, all iodides form hydrogen bonds with Trp or Tyr side chains (Table 7). In cases where the Trp side chain adopts another conformation or other conformations, the atoms of the rotamer hydrogen bonded with an iodide have smaller atomic displacement parameters and occupancies close to those of the iodide.

4. Iodide occupancies

One of our aims in this study was the precise determination of the ion occupancy factors. However, the refinement of partially occupied sites can be difficult, especially in cases where the sites are also occupied by other moieties, such as water. To cross-check that the occupancies of anomalous scatterers are reasonably assigned by conventional refinement, we have carefully analyzed the anomalous signal, which arises mainly from the iodine ions.

Similar issues often appear in macromolecular crystallography in cases of soaking crystals of proteins with heavy-atom derivatives, such as iodides, when several partially occupied sites exist. Thus, we believe that these results are of general interest.

4.1. Analysis of the anomalous signal

The theoretical estimation of the anomalous signal $\Delta_{anom} = \langle|\Delta F|\rangle/\langle F\rangle$ on the basis of the known occupancy factors of I^- and K^+ ions gives a rather small value of about 0.62% at 0.67 Å wavelength (Table 8). The signal was calculated from a formula based on the expression derived by Olczak *et al.* (2003) (see Appendix *A*).

The experimental value of this parameter is much higher, about 1.5%, but it must be remembered that in addition to anomalous differences ΔF_{anom}, the experimental differences ΔF also contain measurement uncertainties ΔF_{err},

$$\Delta F = \Delta F_{anom} + \Delta F_{err}.$$

In summary, the anomalous signal for the studied complex of gramicidin D with KI was rather weak.

4.2. Correlation between iodine occupancy factors and peak heights on the anomalous difference map

Despite the weak anomalous signal, anomalous difference Fourier maps were very helpful in locating iodide ions. In addition to the 0.67 Å wavelength, two additional data sets were collected at wavelengths of 1.466 and 1.77 Å in order to confirm the positions of anomalous scatterers. The maps based on these longer wavelength data sets correlate well with the map obtained from the high-resolution diffraction data. Unfortunately, they do not provide any additional information on the positions of the anomalous scatterers and consequently in the following discussion we have only used the high-resolution data.

The maps (ΔF, $\varphi_{calc} - 90^\circ$) were prepared with phases, φ_{calc}, calculated for the gramicidin structure alone (no water or any other molecules). All eight I^- ions and two of the K^+ ions were identified on these maps. However, the peak heights on these

Table 5
Gramicidin-channel contents in the crystal structure of the gD–KI complex.

(*a*) Channel contents.

	Water		K		I	
	Contents	Sites	Contents	Sites	Contents	Sites
Channel I	8.4 (1)	29	0.50 (1)	3		
Channel II	8.4 (1)	25	0.60 (1)	3		
Outside the channels	10.3 (1)	32			1.095 (7)	8
Total	27.0 (2)	85	1.10 (1)	6	1.095 (7)	8

(*b*) Ratios.

	H_2O/K^+	K/I
Channel I	16.8	
Channel II	14.0	
Overall		1.005

maps correlate poorly with the occupancy factors for the I^- anions determined during refinement (Table 9). The main discrepancy concerns I(25), I(26) and I(27), which were much weaker on the anomalous difference map than might be expected from their occupancy factors. This is because of their high 'temperature' (or delocalization) factors, which cause the spreading of electron density over a larger volume. Indeed, the correlation between peak heights multiplied by the volume of the 'thermal ellipsoids' *versus* occupancy is much better (Fig. 5).

4.3. The Flack parameter as an indicator of the anomalous substructure correctness

During the study of another gramicidin D complex with CsCl (unpublished data), we found that after 'final' refinement the value of the Flack parameter was as high as 0.25 (2). Twinning by inversion was excluded as gramicidin D is a natural product. We found that overestimation of the occupancies of the anomalous scatterers (primarily Cs^+ ions in this case) could be the explanation for the high value of this parameter (see Appendix *B*). For this reason, we decided to check the value of this parameter for the studied complex of gramicidin D with KI.

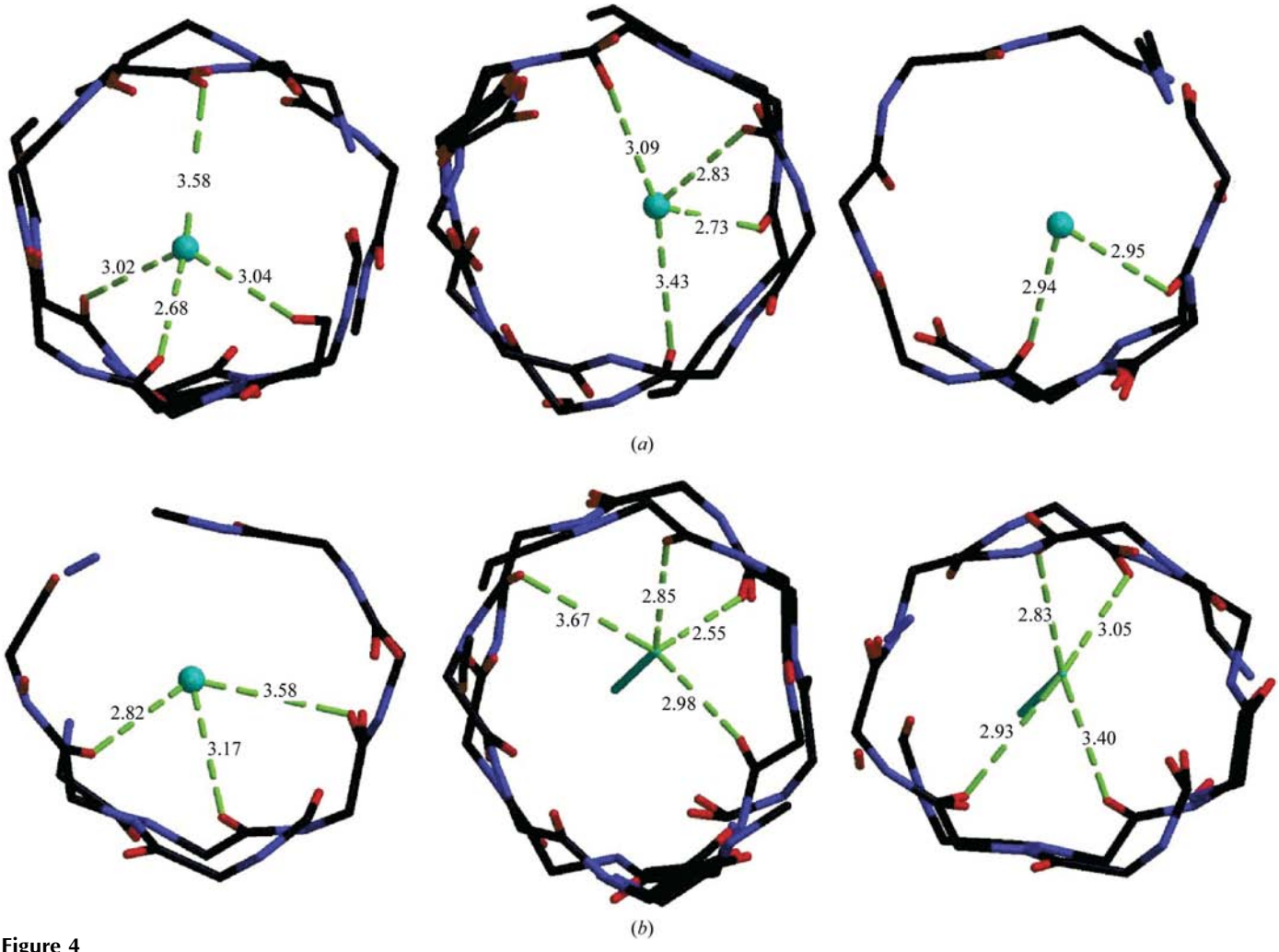

Figure 4
Short $K^+\cdots O$(carbonyl) contacts (below 3.7 Å) viewed along [001] for channels I (*a*) and II (*b*) in the crystal structure of the gD–KI complex.

Table 6
Geometry of K···carbonyl contacts for K···O distances less than 3.7 Å.

The contacts with K—O—C angles of less than 120°, which refer to the cases where a cation interacts with the π-electrons of a carbonyl bond rather than with a lone pair of the O atom, are italicized and respective values in relation to the center of the carbonyl bond (indicated by X) are given. The mean estimated standard deviations of distances and angles are 0.008 Å and 0.5°, respectively.

K	Residue	K—O (Å)	K—O—C (°)	K—C (Å)	K—C—O (°)	K—X (Å)	K—X—O (°)
1	104a	2.684	140.9				
1	210	3.023	132.1				
1	*212*	*3.043*	*98.9*	*3.456*	*60.5*	*3.197*	*70.1*
1	*104b*	*3.511*	*92.1*	*3.784*	*68.0*	*3.593*	*77.6*
1	107b	3.583	*101.3*	*4.013*	*61.1*	*3.753*	*69.4*
2	108	2.730	128.4				
2	206a	2.826	129.8				
2	*110b*	*3.092*	*102.6*	*3.647*	*55.8*	*3.310*	*65.7*
2	*206b*	*3.293*	*100.8*	*3.743*	*59.8*	*3.468*	*68.8*
2	*208*	*3.431*	*91.9*	*3.685*	*68.5*	*3.507*	*77.9*
3	*202*	*2.940*	*100.7*	*3.396*	*58.3*	*3.115*	*68.0*
3	*114*	*2.948*	*112.8*	*3.597*	*49.1*	*3.232*	*57.2*
11	414	2.818	123.4				
11	*302*	*3.174*	*96.3*	*3.518*	*63.7*	*3.296*	*73.2*
11	*303b*	*3.578*	*100.9*	*4.006*	*61.3*	*3.746*	*69.7*
12	406a	2.551	139.7				
12	406b	2.704	127.1				
12	308	2.847	127.7				
12	*310*	*2.976*	*96.7*	*3.355*	*61.8*	*3.110*	*71.9*
12	*408*	*3.666*	*78.9*	*3.635*	*81.9*	*3.600*	*91.5*
13	409a	2.833	121.4				
13	310	2.926	118.1				
13	313a	3.050	122.4				
13	*409b*	*3.289*	*99.6*	*3.666*	*62.2*	*3.433*	*70.8*
13	*406a*	*3.403*	*110.8*	*4.003*	*52.6*	*3.665*	*60.2*
13	*406b*	*3.570*	*102.0*	*4.003*	*60.7*	*3.744*	*68.8*

The Flack parameter was introduced mainly for absolute structure determination in small-molecule crystallography (Flack & Bernardinelli, 1999).

The 'true structure factors' G_{hkl} (or $F_{hkl,\mathrm{true}}$ in the nomenclature adopted here) are calculated as

$$|G_{hkl}|^2 = (1-x)|F_{hkl,\mathrm{model}}|^2 + x|F_{\overline{hkl},\mathrm{model}}|^2 \qquad (1)$$

(where $F_{hkl,\mathrm{model}}$ values are calculated structure factors for a given model) and are compared with the observed values for all measured reflections, so the value of x with a proper standard uncertainty can be estimated ($x \simeq 0$ means that the structure is correct, while $x \simeq 1$ means that the structure should be inverted). Any other value between 0 and 1 indicates possible twinning by inversion.

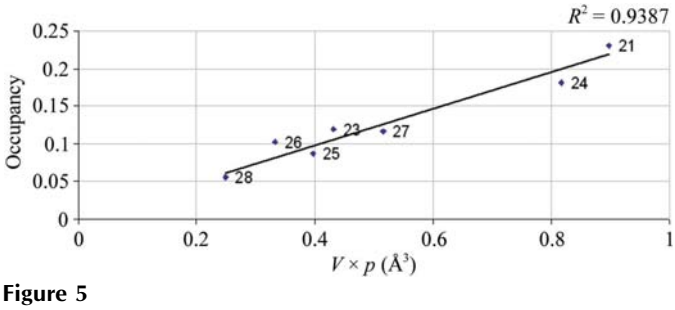

Figure 5
Correlation between $V \times p$ and the occupancy factors of anomalously scattering iodine ions. V is the volume, calculated as $(4/3)\pi(U_{11}U_{22}U_{33})^{1/2}$, where U_{11}, U_{22} and U_{33} are the components of the diagonalized displacement tensor, and p is a maximum on the anomalous difference density map.

Table 7
Geometry of $I^-\cdots$HN (Trp) and $I^-\cdots$HO (Tyr) contacts (distances less than 4.50 Å).

The restraints were imposed on distances and angles with estimated standard deviations of 0.02 Å and 1.5°, respectively.

I	Atom	Distance (Å)	HE1 (Å)	Angle (°)
21	Trp313 NE1	3.89	3.27	131.8
	Trp115 NE1	3.61	2.85	149.3
	Trp113NE1	3.72	3.18	123.1
	Trp209a NE1	3.81	3.06	148.4
22	Trp313 NE1	3.75	3.07	138.4
	Trp113 NE1	4.01	3.54	117.3
	Trp115 NE1	3.49	2.75	144.4
	Trp209a NE1	3.39	2.63	148.7
23	Trp315a NE1	3.37	2.66	140.4
	Trp409b NE1	3.82	3.07	147.0
	Trp313 NE1	4.25	3.80	115.8
	Trp115 NE1	3.48	2.93	123.9
	Trp113 NE1	3.61	2.85	147.5
24	Trp311 NE1	3.66	2.86	157.3
	Tyr1311 OH	3.85	3.07	160.0
25	Trp413a NE1	3.60	2.77	164.1
	Trp415a NE1	4.03	3.29	145.7
	Trp415b NE1	3.99	3.35	133.7
	Tyr1211 OH	3.46	3.10	109.5
26	Trp411 NE1	3.82	2.97	168.6
	Trp213a NE1	3.53	2.73	154.6
	Trp213b NE1	3.64	3.25	110.9
	Tyr1411 OH	4.00	3.25	168.7
27	Trp411 NE1	3.40	2.65	146.1
	Trp213a NE1	3.61	2.78	162.7
	Trp213b NE1	3.85	3.25	129.1
28	Trp209b NE1	3.92	3.18	146.6

In protein crystallography, where the absolute structure of molecules is unambiguous, the Flack parameter should always be equal to zero (when the anomalous signal is sufficiently strong). If it is not, as in the case of the gD–CsCl complex mentioned above, it can be used as a test for the correctness of the overall occupancy of anomalously scattering atoms. This is because rescaling the occupancy factors of all anomalously scattering atoms by a common factor, say α [$\Delta|F|^2_{\mathrm{anom,true}} = (1/\alpha)\Delta|F|^2_{\mathrm{anom,model}}$], has the same effect on anomalous differences as twinning by inversion with the Flack parameter x [$\Delta|F|^2_{\mathrm{anom,true}} = (1-2x)\Delta|F|^2_{\mathrm{anom,model}}$] and consequently $1-2x = 1/\alpha$ (see Appendix *B*).

When there is no doubt about the chirality of a given structure, a significantly positive value of the Flack parameter may indicate that the total occupancy of the anomalous substructure is overestimated and a significantly negative value may indicate that it is underestimated.

The final value of the Flack parameter in this study is 0.032 (14). This value is low (close to zero) and precise enough to confirm the correctness of the anomalous substructure.

5. Conclusions

The composition of the gramicidin in the crystal studied was 67.25% gA, 6.75% gB and 26% gC, which was visibly different from the composition of the starting material (gramicidin D)

Table 8
Anomalous corrections f', f'' to atomic scattering factors (Kissel *et al.*, 1995) and calculated anomalous signal contributions from K, I and K–I cross-terms.

λ (Å)	$f'_{\rm K}$	$f''_{\rm K}$	$f'_{\rm I}$	$f''_{\rm I}$	$\Delta^{\rm K}_{\rm anom}$ (%)	$\Delta^{\rm I}_{\rm anom}$ (%)	$\Delta^{\rm KI}_{\rm anom}$ (%)	$\Delta_{\rm anom}$ (%)
0.670	0.186	0.225	−0.535	1.652	0.08	0.61	0.02	0.62
1.466	0.385	0.978	−0.143	6.334	0.35	2.33	0.07	2.36
1.770	0.358	1.362	−0.972	8.592	0.49	3.18	0.10	3.22

Table 9
Occupancy factors of all iodine ions, equivalent atomic displacement parameters B, volumes of thermal ellipsoids V, peak heights on the anomalous difference Fourier map p (at 0.67 Å wavelength; arbitrary units) and the product of V and p.

The p value for I(22) is absent owing to the overlap of I(22) and I(21).

Ion	Occupancy	B (Å^2)	V (Å^3)	p	$p \times V$ (Å^3)
I(21)	0.231	4.68	0.0139	64.44	0.90
I(22)	0.203	5.53			
I(23)	0.119	6.94	0.0241	17.89	0.43
I(24)	0.181	8.01	0.0295	27.65	0.82
I(25)	0.087	11.34	0.0498	7.98	0.40
I(26)	0.102	11.46	0.0421	7.91	0.33
I(27)	0.116	10.78	0.0436	11.83	0.52
I(28)	0.056	9.62	0.0346	7.17	0.25

used in crystallization, which contained about 80% gA, 5% gB and 15% gC. In addition, the gB component has been found only in one strand of each crystallographically independent gramicidin dimer, in amounts of 12% and 15%, resulting in their asymmetry.

The distributions of K^+ sites and their occupancies in the two crystallographically independent channels were asymmetrical, which correlates with the asymmetry of gramicidin dimers. Surprisingly, the overall content of potassium was low (about 0.50 in dimer I and 0.60 in dimer II). The values were in accord with the content of the counterion iodide (1.095), which is confirmed unequivocally by its anomalous signal.

The Flack parameter can be helpful in detecting inaccuracies in occupancy parameters of the anomalous substructure.

APPENDIX *A*

For the structure factor $F_{hkl} = \sum_{j=1}^{N} f_j \exp(2\pi i \mathbf{H}\cdot\mathbf{r}_j)$, the following formula expresses the anomalous intensity difference (Olczak *et al.*, 2003),

$$\Delta|F|^2_{\rm anom} = -4\sum_{k=1}^{N}\sum_{j>k}^{N} f_{oj}f_{ok}\sin\Delta_{jk}\sin(2\pi\mathbf{H}\cdot\Delta\mathbf{r}_{jk}), \quad (2)$$

where $\Delta\mathbf{r}_{jk} = \mathbf{r}_j - \mathbf{r}_k$, $\Delta_{jk} = = \delta_j - \delta_k$ and $f_j = f_{oj}\exp(i\delta_j)$.

It can be seen that taking into account partial occupancy and thermal vibrations, this formula can be generalized as

$$\Delta|F|^2_{\rm anom} = -4\sum_{k=1}^{N}\sum_{j>k}^{N}\exp(-T_j)\exp(-T_k)c_jc_kf_{oj}f_{ok} \times \sin\Delta_{jk}\sin(2\pi\mathbf{H}\cdot\Delta\mathbf{r}_{jk}), \quad (3)$$

where $\exp(-T_i) = \exp(-B_i\sin^2\theta/\lambda^2)$ for $i = j, k$ and c_j and c_k are occupancy factors.

However, because we are interested in estimating the magnitude of the anomalous signal at the low-resolution limit ($\sin^2\theta/\lambda^2 \rightarrow 0$) we can safely neglect $\exp(-T_i)$ terms. Following consideration presented in Olczak *et al.* (2003), we can conclude that the anomalous signal $\Delta_{\rm anom} = \langle|\Delta F|\rangle/\langle F\rangle$, which comes from K and I ions, can be expressed as

$$\Delta_{\rm anom} = [(\Delta^{\rm K}_{\rm anom})^2 + (\Delta^{\rm I}_{\rm anom})^2 + (\Delta^{\rm KI}_{\rm anom})^2]^{1/2}, \quad (4)$$

where

$$\Delta^{\rm K}_{\rm anom} = \frac{8}{\pi^{3/2}}\frac{|f''_{\rm K}(f_{\rm L}+f'_{\rm L}) - f''_{\rm L}(f_{\rm K}+f'_{\rm K})|}{\langle|F|^2\rangle}\left(N_{\rm L}\sum_{i=1}^{N_{\rm K}}c^2_{{\rm K}_i}\right)^{1/2}, \quad (5)$$

$$\Delta^{\rm I}_{\rm anom} = \frac{8}{\pi^{3/2}}\frac{|f''_{\rm I}(f_{\rm L}+f'_{\rm L}) - f''_{\rm L}(f_{\rm I}+f'_{\rm I})|}{\langle|F|^2\rangle}\left(N_{\rm L}\sum_{i=1}^{N_{\rm I}}c^2_{{\rm I}_i}\right)^{1/2}, \quad (6)$$

$$\Delta^{\rm KI}_{\rm anom} = \frac{8}{\pi^{3/2}}\frac{|f''_{\rm I}(f_{\rm K}+f'_{\rm K}) - f''_{\rm K}(f_{\rm I}+f'_{\rm I})|}{\langle|F|^2\rangle}\left(\sum_{j=1}^{N_{\rm K}}\sum_{i=1}^{N_{\rm I}}c^2_{{\rm K}_j}c^2_{{\rm I}_i}\right)^{1/2}, \quad (7)$$

and

$$\langle|F|^2\rangle = f^2_{o{\rm K}}\sum_{i=1}^{N_{\rm K}}c^2_{{\rm K}_i} + f^2_{o{\rm I}}\sum_{i=1}^{N_{\rm I}}c^2_{{\rm I}_i} + N_{\rm L}f^2_{o{\rm L}},$$

where $N_{\rm K}$, $N_{\rm I}$ and $N_{\rm L}$ are the numbers of potassium, iodine and light-atom (C, N, O) sites, respectively. More accurate calculations, where all atoms in a given structure are treated as anomalous scatterers, can be carried out on a web page http://alfa.p.lodz.pl/anomal (Sieron, 2006).

Note added in proof: at the proofreading stage we learnt about a forthcoming paper by Flack & Shmueli (2007), in which a very detailed analysis of the anomalous signal, in more general case of partialy centrosymmetric structures, is presented.

APPENDIX *B*

Using the definition of G_{hkl} (1), the following formula for the appropriate anomalous difference can be derived:

$$\Delta|G|^2 \equiv \Delta|F|^2_{\rm anom,true} = (1-2x)\Delta|F|^2_{\rm anom,model} \quad (8)$$

where $\Delta|F|^2_{\rm anom,true}$ are the ideal anomalous differences to which experimental values should be compared and $\Delta|F|^2_{\rm anom,model}$ are the calculated anomalous differences for a given model.

On the other hand, using (3) we can write the anomalous difference in the case of one type of anomalous scatterer (for the sake of simplicity) in the form

$$\Delta|F|^2_{\rm anom,true} = -4\sum_{k=1}^{N}\sum_{j>k}^{N}\exp(-T_j)\exp(-T_k)c_{A_j}f_{oj}f_{ok} \times \sin\Delta_{jk}\sin(2\pi\mathbf{H}\cdot\Delta\mathbf{r}_{jk}). \quad (9)$$

If, for some reason, incorrect occupancy parameters $c'_{A_j} = \alpha c_{A_j}$ are used in our model instead of the correct ones (c_{A_j}), new

anomalous differences $\Delta|F|^2_{\rm anom,model}$ can be expressed in the form

$$\Delta|F|^2_{\rm anom,model} = -4\alpha \sum_{k=1}^{N}\sum_{j>k}^{N} \exp(-T_j)\exp(-T_k)c_{A_j}f_{oj}f_{ok} \times \sin\Delta_{jk}\sin(2\pi\mathbf{H}\cdot\Delta\mathbf{r}_{jk}) \quad (10)$$

and consequently

$$\Delta|F|^2_{\rm anom,model} = \alpha\Delta|F|^2_{\rm anom,true}. \quad (11)$$

Comparing (8) and (11), one can conclude that

$$1-2x = (1/\alpha). \quad (12)$$

In the case of many types of anomalous scatterers, (11) becomes more complicated because of cross-terms between anomalous scatterers of different types (the third term in the expression below),

$$\begin{aligned}\Delta|F|^2_{\rm anom,model} = &-4\alpha \sum_{k=1}^{N}\sum_{j>k}^{N} \exp(-T_j)\exp(-T_k)c_{A_j}f_{oj}f_{ok} \times \sin\Delta_{jk}\sin(2\pi\mathbf{H}\cdot\Delta\mathbf{r}_{jk}) \\ &-4\alpha \sum_{k=1}^{N}\sum_{j>k}^{N} \exp(-T_j)\exp(-T_k)c_{B_j}f_{oj}f_{ok} \times \sin\Delta_{jk}\sin(2\pi\mathbf{H}\cdot\Delta\mathbf{r}_{jk}) \\ &-4\alpha^2 \sum_{k=1}^{N}\sum_{j>k}^{N} \exp(-T_j)\exp(-T_k)c_{A_j}c_{B_j}f_{oj}f_{ok} \times \sin\Delta_{jk}\sin(2\pi\mathbf{H}\cdot\Delta\mathbf{r}_{jk}). \end{aligned} \quad (13)$$

Fortunately, in this study the cross-terms (between potassium and iodine) are very small and can be neglected.

However, a word of caution is needed here. The use of the Flack parameter to judge the correctness of the anomalous substructure should not be treated as completely decisive because the parameter may be adversely influenced by inaccuracies in the estimation of the measured anomalous differences and by inaccuracies in several other structural parameters within the model.

In summary, the above considerations suggest that for difficult cases (when the occupancy parameters of anomalous scatterers are ambiguous) and when the anomalous substructure is a small part of the whole structure (which means that freely refined occupancy parameters of anomalous scatterers have little influence on the total structure factors), anomalous differences can be helpful in assignment of proper occupancy factors to these scatterers.

Moreover, refinement of occupancy parameters of the anomalously scattering atoms (when the rest of the structure is precisely determined) based on anomalous differences could probably provide better estimates for these parameters. This refinement could be performed on the basis of the equation

$$R_{\Delta F_{\rm anom}} = \frac{\sum_{hkl} w_{hkl}(\Delta F^{\rm o}_{hkl} - \Delta F^{\rm c}_{hkl})^2}{\sum_{hkl} w_{hkl}(\Delta F^{\rm o}_{hkl})^2}, \quad (14)$$

where $\Delta F^{\rm o}$ and $\Delta F^{\rm c}$ are the observed and calculated anomalous differences, respectively.

This paper owes much to the helpful comments of referees and the Editor (Z. Dauter) and we take pleasure in acknowledging this assistance. Financial support from the Polish Committee for Scientific Research under project 3 T09A 047 26 (2004–2006) and the Institute of General and Ecological Chemistry (PB-DS 47) is also gratefully acknowledged. The use of the Advanced Photon Source was supported by the US Department of Energy, Basic Energy Sciences, Office of Energy Research under Contract No. W-31-102-Eng-38.

References

Berman, H. M., Westbrook, J., Feng, Z., Gilliland, G., Bhat, T. N., Weissig, H., Shindyalov, I. N. & Bourne, P. E. (2000). *Nucleic Acids Res.* **28**, 235–242.
Burkhart, B. M., Gassman, R. M., Langs, D. A., Pangborn, W. A. & Duax, W. L. (1998). *Biophys. J.* **75**, 2135–2146.
Burkhart, B. M., Gassman, R. M, Langs, D. A., Pangborn, W. A., Duax, W. L. & Pletnev, V. (1999). *Biopolymers*, **51**, 129–144.
Burkhart, B. M., Li, N., Langs, D. A., Pangborn, W. A. & Duax, W. L. (1998). *Proc. Natl Acad. Sci. USA*, **95**, 12950–12955.
Collaborative Computational Project, Number 4 (1994). *Acta Cryst.* D**50**, 760–763.
Doyle, D. A. & Wallace, B. A. (1997). *J. Mol. Biol.* **266**, 963–977.
Duax, W. L., Pletnev, V. & Burkhart, B. M. (2003). *J. Mol. Struct.* **647**, 97–111.
Engh, R. A. & Huber, R. (1991). *Acta Cryst.* A**47**, 392–400.
Flack, H. D. & Bernardinelli, G. (1999). *Acta Cryst.* A**55**, 908–915.
Flack, H. D. & Shmueli, U. (2007). *Acta Cryst.* A**63**. In the press.
Główka, M. L, Olczak, A., Bojarska, J., Szczesio, M., Duax, W. L., Burkhart, B. M., Pangborn, W. A., Langs, D. A. & Wawrzak, Z. (2005). *Acta Cryst.* D**61**, 433–441.
Hotchkiss, R. D. (1944). *Adv. Enzymol.* **4**, 153–199.
Hladky, S. B. & Haydon, D. A. (1970). *Nature (London)*, **225**, 451–453.
Kissel, L., Zhou, B., Roy, S. C., Sen Gupta, S. K. & Pratt, R. M. (1995). *Acta Cryst.* A**51**, 271–288.
Langs, D. A. (1988). *Science*, **241**, 188–191.
Langs, D. A., Smith, G. D., Courseille, C., Précigoux, G. & Hospital, M. (1991). *Proc. Natl Acad. Sci. USA*, **88**, 5345–5349.
Laskowski, R. A., MacArthur, M. W., Moss, D. S. & Thornton, J. M. (1993). *J. Appl. Cryst.* **26**, 283–291.
McRee, D. E. (1999). *J. Struct. Biol.* **125**, 156–165.
Merritt, E. A. & Murphy, M. E. P. (1994). *Acta Cryst.* D**50**, 869–873.
Olczak, A., Cianci, M., Hao, Q., Rizkallah, P. J., Raftery, J. & Helliwell, J. R. (2003). *Acta Cryst.* A**59**, 327–334.
Otwinowski, Z. & Minor, W. (1997). *Methods Enzymol.* **276**, 307–326.
Roux, B. & Karplus, M. (1994). *Annu. Rev. Biophys. Biomol. Struct.* **23**, 731–761.
Sarges, R. & Witkop, B. (1965). *J. Am. Chem. Soc.* **87**, 2011–2020.
Sheldrick, G. M. & Schneider, T. R. (1997). *Methods Enzymol.* **277**, 319–343.
Sieron, L. (2006). Personal communication.
Urry, D. W. (1971). *Proc. Natl Acad. Sci. USA*, **68**, 672–676.
Wallace, B. A., Hendrickson, W. A. & Ravikumar, K. (1990). *Acta Cryst.* B**46**, 440–446.
Wallace, B. A. & Ravikumar, K. (1988). *Science*, **241**, 182–187.
Weinstein, S., Wallace, B. A., Morrow, J. S. & Veatch, W. R. (1980). *J. Mol. Biol.* **143**, 1–19.